

Inhomogeneous longitudinal electric field-induced anomalous Hall conductivity in a ferromagnetic two-dimensional electron gas

Ankur Sensharma^{1,2} and Sudhansu S. Mandal¹

¹*Department of Theoretical Physics, Indian Association for the Cultivation of Science, Jadavpur, Kolkata 700 032, India*

²*Department of Physics, University of Gour Banga, Malda 732101, West Bengal, India*

(Dated: October 30, 2018)

It is known that the anomalous Hall conductivity (AHC) in a disordered two dimensional electron system with Rashba spin-orbit interaction and finite ferromagnetic spin-exchange energy is zero in the metallic weak-scattering regime because of the exact cancellation of the bare-bubble contribution by the vertex correction. We study the effect of inhomogeneous longitudinal electric field on the AHC in such a system. We predict that AHC increases from zero (at zero wavenumber), forms a peak, and then decreases as the wavenumber for the variation of electric field increases. The peak-value of AHC is as high as the bare-bubble contribution. We find that the wave number, q , at which the peaks occur is the inverse of the geometric mean of the mean free path of an electron and the spin-exchange length scale. Although the Rashba energy is responsible for the peak-value of AHC, the peak position is independent of it.

PACS numbers: 72.15.Eb, 72.20.Dp, 72.25.-b

I. INTRODUCTION

Hall resistance in a ferromagnetic material is known to have two contributions: 1) proportional to magnetic field, 2) proportional to magnetization. While the former is responsible for conventional Hall effect, the latter is due to anomalous Hall effect (AHE). The anomalous Hall coefficient is the zero field Hall resistance which is estimated by extrapolating Hall resistance up to zero magnetic field. The physical mechanisms which contribute to the anomalous Hall conductivity (AHC), are broadly categorized into two classes: intrinsic and extrinsic. While the properties of the bands are responsible for the former, the spin dependent scattering of electrons belong to the extrinsic mechanism. Karplaus and Luttinger¹ proposed intrinsic mechanism due to the spin-orbit interaction (SOI) for the polarized electrons in ferromagnetic materials. This mechanism was later realized as the outcome of the Berry phase² from band topology. Smit³ proposed an extrinsic mechanism which is known as ‘skew-scattering’ (SS) in which electrons scatter from impurities with spin asymmetry. In addition, contribution due to side-jump (SJ) scattering was put forward by Berger⁴ through a semi-classical theory.

The debate on the true mechanism for AHE grew stronger with the contradicting results⁵ for various systems. The linear transport theories, which are now mostly used to study AHE, seem to have settled some of the confusing issues in the recent years. Although, different approaches of this theory often tend to conflict with each other, there are some successful attempts^{6,7} to establish links between them. To this end, the two dimensional ferromagnetic-Rashba gas, *i.e.*, electrons with Rashba SOI and ferromagnetic exchange coupling has proved to be a simple and elegant model to work with because it captures almost all the important and fundamental features relevant to AHE. Due to the Rashba

SOI, characterized by the Rashba energy Δ_R , degeneracy is lifted by the formation of two chiral subbands with opposite helicity. Further, ferromagnetic spin-exchange energy produces a gap between these subbands.

A number of studies on AHC have been performed within the model of two-dimensional ferromagnetic-Rashba gas, using the Kubo formalism^{6,8-14}, the Keldysh technique^{6,15,16}, and the semiclassical treatment of Boltzmann transport equation^{17,18}. According to the studies in Kubo formalism, the magnitude of AHC is sensitive to whether only one or both the subbands are occupied by the electrons, *i.e.*, whether or not the Fermi level is situated below the band-gap created by exchange energy, Δ_{ex} . In the presence of non-magnetic impurities, both the Fermi sea and Fermi surface contributions in AHC vanish¹¹ when $\epsilon_F > \Delta_{ex}$, where ϵ_F is the Fermi energy. The bare-bubble contribution is exactly canceled by the vertex correction^{10,11} due to SJ mechanism, and the SS term is absent¹². On the contrary, all these terms are finite for $\epsilon_F < \Delta_{ex}$. A comprehensive analysis of these works can be found in the detailed study of Nunner *et al*¹¹. Using the Keldysh technique in a T-matrix approximation, Onoda *et al*^{15,19}, however, find a strong SS contribution that leads to non-zero AHC even when $\epsilon_F > \Delta_{ex}$. They also observe that the AHC changes sign when the Fermi level enters into the band gap. The Keldysh technique automatically incorporates the higher order Born scatterings and enables them to arrive at such striking conclusions when the Fermi energy is located around the anticrossing of band dispersions in momentum space. Kovalev *et al*¹⁶ later included the higher order scatterings explicitly in the Kubo formalism to match the results of Onoda *et al*¹⁵ and were able to unify the these approaches⁷ at least for a certain range of parameters.

There is no controversy, however, in the metallic weak-scattering regime ($\epsilon_F \tau > 1$), where τ is the mean scattering time of an electron. When the Fermi level goes far above the band gap ($\epsilon_F > \Delta_{ex}$), *i.e.*, when both the

chiral subbands are occupied, the AHC vanishes^{5,7,11,20}, making this regime a somewhat uninteresting one. We however note that AHE is intimately related to spin hall effect^{21,22} and there are instances of enhancement of spin-Hall conductivity²³ and occurrence of a induced transverse force²⁴ due to inhomogeneity of the applied electric field. In this paper, we study the effect of inhomogeneous longitudinal electric field ($\mathbf{E}_q \parallel \mathbf{q}$) on the AHC in the metallic weak-scattering regime when both the subbands are occupied.

We find, within the Kubo formalism, that AHC, σ^{AH} , is zero at $q = 0$, increases with q and forms a peak at certain q before it decreases to zero at large q . σ^{AH} depends on the parameters $\epsilon_F \tau$, $\Delta_{ex} \tau$, and $\Delta_R \tau$. We find that the peak-value of AHC is proportional to $(\Delta_R \tau)^2 (\epsilon_F \tau)^{-1}$ and the peak occurs when $ql_{eff} \approx 1$, where $l_{eff} = (l_{ex})^{1/2}$, l is the mean free path of an electron, and $l_{ex} = v_F / (4\Delta_{ex})$ is the length-scale corresponding to spin-exchange, with v_F being the Fermi velocity. We note that the momentum at which the peaks occur does not depend on Δ_R .

The paper is organized as follows. The following section contains a brief formalism for the evaluation of the anomalous Hall conductivity. In Section III, we present our results and discuss about the relevant scales and limits. Finally, we summarize our results in Section IV.

II. ANOMALOUS HALL CONDUCTIVITY

A. The model

A system of spin-polarized two dimensional electron gas with Rashba spin-orbit interaction in a disordered environment may be expressed by the Hamiltonian

$$H = \left(\frac{\vec{\nabla}^2}{2m} + V(r) \right) \sigma_0 + \alpha (\vec{\sigma} \times \vec{\nabla}) \cdot \hat{z} - \Delta_{ex} \sigma_z, \quad (1)$$

where m is the the effective mass of an electron, α is the Rashba spin-orbit coupling parameter, Δ_{ex} is the exchange energy which favors one kind of spin over the other, $\vec{\sigma}$ represents three Pauli matrices and σ_0 is 2×2 unit matrix. Here $V(\mathbf{r})$ is the spin independent disorder potential for the randomly located δ -function impurities and has the form $V(\mathbf{r}) = \sum_i V_i \delta(\mathbf{r} - \mathbf{R}_i)$ satisfying $\langle V_i \rangle = 0$, $\langle V_i^2 \rangle = V_2 \neq 0$ and $\langle V_i^3 \rangle = V_3 \neq 0$. (We have set the unit $\hbar = 1$ and $c = 1$.)

In the absence of disorder, the above Hamiltonian can be exactly solved with the eigen values

$$E_k^s = \frac{k^2}{2m} + s\zeta_k \quad (2)$$

where k is the momentum of an electron, $s = \pm$ is the label for two chiral subbands produced due to Rashba spin-orbit interaction and $\zeta_k = \sqrt{\Delta_{ex}^2 + \alpha^2 k^2}$. The corresponding Fermi momenta K_s are given by

$$K_s^2 = 2m [\epsilon_F - s\zeta_s] \quad (3)$$

where ϵ_F is the Fermi energy and

$$\zeta_s = \sqrt{\Delta_{ex}^2 + \Delta_R^2 + m^2 \alpha^4} - s m \alpha^2, \quad (4)$$

with $\Delta_R = \alpha \sqrt{2m\epsilon_F} = \alpha k_F$. Here k_F is the mean Fermi momentum, given by $\epsilon_F = \frac{k_F^2}{2m}$. The density of states at the Fermi level for the two subbands are

$$\nu_s = \nu_0 \left[1 - s \frac{m\alpha^2}{\sqrt{\Delta_{ex}^2 + \Delta_R^2 + m^2 \alpha^4}} \right]. \quad (5)$$

where ν_0 is the density of states for each spin in pure two dimensional electron gas. The free retarded (advanced) Green's function of the system can then be expressed as

$$\hat{G}_{\mathbf{k},0}^{R,A}(\epsilon) = \frac{1}{2} \sum_{s=\pm} \frac{\sigma_0 + s\alpha(\boldsymbol{\sigma} \times \mathbf{k}) \cdot \hat{z} - \Delta_{ex} \sigma_z}{\epsilon - \xi_{\mathbf{k}}^s \pm i\eta}, \quad (6)$$

where $\xi_{\mathbf{k}}^s = E_{\mathbf{k}}^s - \epsilon_F$. The self energy for the electrons due to scattering is then found to be

$$\Sigma^{R(A)} = \mp \frac{i}{4\tau\nu_0} \left[(\nu_+ + \nu_-) \sigma_0 - \Delta_{ex} \left(\frac{\nu_+}{\zeta_+} - \frac{\nu_-}{\zeta_-} \right) \sigma_z \right] \quad (7)$$

in Born approximation, where $\tau = (2\pi\nu_0 n_i V_2)^{-1}$ is the mean scattering time for an electron, and n_i represents the concentration of impurity. We thus find the disorder-averaged Greens functions as

$$\hat{G}_{\mathbf{k}}^R(\epsilon) = \frac{1}{2} \sum_{s=\pm} \frac{\sigma_0 + s\alpha(\boldsymbol{\sigma} \times \mathbf{k}) \cdot \hat{z} - \tilde{\Delta}_{ex} \sigma_z}{\tilde{\epsilon} - \tilde{\xi}_{\mathbf{k}}^s} / \tilde{\zeta}_k, \quad (8)$$

where $\tilde{\epsilon} = \epsilon + i(\nu_+ + \nu_-)/(4\tau\nu_0)$ and $\tilde{\Delta}_{ex} = \Delta_{ex} \left[1 + \frac{i}{4\tau\nu_0} \left(\frac{\nu_+}{\zeta_+} - \frac{\nu_-}{\zeta_-} \right) \right]$. Here $\xi_{\mathbf{k}}^s$ and ζ_k get renormalized to $\tilde{\xi}_{\mathbf{k}}^s$ and $\tilde{\zeta}_k$ due to the presence of $\tilde{\Delta}_{ex}$ instead of Δ_{ex} in their respective expressions. When both the helicity subbands are occupied, $\nu_+ + \nu_- = 2\nu_0$ and $\nu_+/\zeta_+ = \nu_-/\zeta_-$ and therefore exchange energy does not get renormalized and $\tilde{\epsilon}$ becomes $\epsilon + i/2\tau$.

B. Kubo Formula

Using Kubo formula, anomalous Hall conductivity may be expressed as

$$\sigma_{yx}^{AH} = \frac{1}{2\pi} \int \frac{d\mathbf{k}}{(2\pi)^2} \text{Tr} \left[\hat{j}_y \left(\mathbf{k} + \frac{\mathbf{q}}{2} \right) \hat{G}_{\mathbf{k}+\mathbf{q}}^R(0) \times \left\{ \hat{j}_x \left(\mathbf{k} + \frac{\mathbf{q}}{2} \right) + \hat{\Gamma}_x(\mathbf{q}) \right\} \hat{G}_{\mathbf{k}}^A(0) \right] \quad (9)$$

where charge current operators $\hat{j}_x(\mathbf{k}) = e(\frac{k_x}{m}\sigma_0 - \alpha\sigma_y)$ and $\hat{j}_y(\mathbf{k}) = e(\frac{k_y}{m}\sigma_0 + \alpha\sigma_x)$, and $\hat{\Gamma}_x(\mathbf{q})$ represents the correction to the vertex of \hat{j}_x due to both side-jump and skew scattering contributions (see fig.1) which can be calculated by solving the self-consistent equation

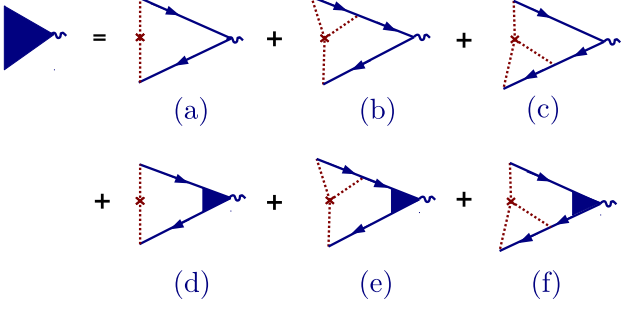


FIG. 1. (Color online) Diagrammatic representation of the self-consistent equation [10] including side-jump (ladder) and skew-scattering corrections. The small wavy lines with a point vertex represent the bare charge current vertex \hat{j}_x , and the small wave lines with dressed vertex represent $\hat{\Gamma}_x$. Retarded and advanced Green's functions are represented by the solid lines with arrows in the opposite directions. Dashed lines refer to the impurity scattering. Lowest order side-jump (a) and skew-scattering (b,c) diagrams; diagrams (d,e,f) represent vertex correction to the diagrams (a,b,c) respectively. Here vertex correction due to both side-jump and skew-scattering.

$$\begin{aligned}
\hat{\Gamma}_x(\mathbf{q}) = & \gamma_1 \int \frac{d\mathbf{k}'}{(2\pi)^2} \hat{G}_{\mathbf{k}'+\mathbf{q}}^R(0) \left[\hat{j}_x\left(\mathbf{k}' + \frac{\mathbf{q}}{2}\right) + \hat{\Gamma}_x(\mathbf{q}) \right] \hat{G}_{\mathbf{k}'}^A(0) \\
& + \gamma_2 \int \frac{d\mathbf{k}'}{(2\pi)^2} \hat{G}_{\mathbf{k}'+\mathbf{q}}^R \int \frac{d\mathbf{k}''}{(2\pi)^2} \hat{G}_{\mathbf{k}''+\mathbf{q}}^R \\
& \quad \times \left[\hat{j}_x\left(\mathbf{k}'' + \frac{\mathbf{q}}{2}\right) + \hat{\Gamma}_x(\mathbf{q}) \right] \hat{G}_{\mathbf{k}''}^A(0) \\
& + \gamma_2 \int \frac{d\mathbf{k}''}{(2\pi)^2} \hat{G}_{\mathbf{k}''+\mathbf{q}}^R(0) \left[\hat{j}_x\left(\mathbf{k}'' + \frac{\mathbf{q}}{2}\right) + \hat{\Gamma}_x(\mathbf{q}) \right] \\
& \quad \times \hat{G}_{\mathbf{k}''}^A(0) \int \frac{d\mathbf{k}'}{(2\pi)^2} \hat{G}_{\mathbf{k}'}^A(0), \tag{10}
\end{aligned}$$

where, $\gamma_1 = n_i V_2$ and $\gamma_2 = n_i V_3$. It is established from a number of studies^{6,11,12} that the skew-scattering contribution to the homogeneous ($q = 0$) anomalous Hall conductivity vanishes provided both the chiral subbands are occupied. This, however, is true for any q since the last two terms in Eq.(10) cancel each other because of the identity $\int \frac{d\mathbf{k}}{(2\pi)^2} \hat{G}_{\mathbf{k}}^{R,A} = \mp i\pi\nu_0\sigma_0$. Equation (9) therefore reduces to

$$\begin{aligned}
\sigma_{yx}^{AH} = & \frac{1}{2\pi} \int \frac{d\mathbf{k}}{(2\pi)^2} \text{Tr} \left[\hat{j}_y\left(\mathbf{k} + \frac{\mathbf{q}}{2}\right) \hat{G}_{\mathbf{k}+\mathbf{q}}^R(0) \right. \\
& \left. \times \left\{ \hat{j}_x\left(\mathbf{k} + \frac{\mathbf{q}}{2}\right) + \hat{J}_x(\mathbf{q}) \right\} \hat{G}_{\mathbf{k}}^A(0) \right] \tag{11}
\end{aligned}$$

with $\hat{J}_x(\mathbf{q})$ containing side-jump types of scattering contribution of $\hat{\Gamma}_x(\mathbf{q})$ only, *i.e.*,

$$\begin{aligned}
\hat{J}_x(\mathbf{q}) = & \frac{1}{2\pi\nu_0\tau} \int \frac{d\mathbf{k}'}{(2\pi)^2} \hat{G}_{\mathbf{k}'+\mathbf{q}}^R(0) \left\{ \hat{j}_x\left(\mathbf{k}' + \frac{\mathbf{q}}{2}\right) \right. \\
& \left. + \hat{J}_x(\mathbf{q}) \right\} \hat{G}_{\mathbf{k}'}^A(0). \tag{12}
\end{aligned}$$

We numerically evaluate $\hat{J}_x(\mathbf{q})$ and hence σ_{yx}^{AH} below.

C. Numerical evaluation

The numerical evaluation of σ_{yx}^{AH} via Eqs. (11) and (12) proceeds with the same spirit of Refs. 14 and 23. Expanding $\hat{J}_x(\mathbf{q})$ in the Pauli matrix basis: $\hat{J}_x = \sum_{\alpha=0}^3 J_{\alpha}\sigma_{\alpha}$, Eq.(12) can be rewritten as

$$\begin{aligned}
\sum_{\alpha} J_{\alpha}(\mathbf{q})\sigma_{\alpha} - \frac{1}{2\pi\nu_0\tau} \int \frac{d\mathbf{k}}{(2\pi)^2} \hat{G}_{\mathbf{k}+\mathbf{q}}^R(0) \left(\sum_{\alpha} J_{\alpha}(\mathbf{q})\sigma_{\alpha} \right) \\
\times \hat{G}_{\mathbf{k}}^A(0) = \frac{1}{2\pi\nu_0\tau} \int \frac{d\mathbf{k}}{(2\pi)^2} \hat{G}_{\mathbf{k}+\mathbf{q}}^R(0) \hat{j}_x\left(\mathbf{k} + \frac{\mathbf{q}}{2}\right) \hat{G}_{\mathbf{k}}^A(0). \tag{13}
\end{aligned}$$

Equating the coefficients of the four Pauli matrices in the above equation, we find a 4×4 matrix equation:

$$\begin{pmatrix} 1 - m_{00} & -m_{11} & -m_{22} & -m_{33} \\ -m_{01} & 1 - m_{10} & im_{23} & -im_{32} \\ -m_{02} & -im_{13} & 1 - m_{20} & im_{31} \\ -m_{03} & im_{12} & -im_{21} & 1 - m_{30} \end{pmatrix} \begin{pmatrix} J_0 \\ J_1 \\ J_2 \\ J_3 \end{pmatrix} = \begin{pmatrix} z_0 \\ z_1 \\ z_2 \\ z_3 \end{pmatrix}, \tag{14}$$

where $m_{\alpha\beta}(\mathbf{q})$ and $z_{\beta}(\mathbf{q})$ are given by²⁵

$$\sum_{\beta=0}^3 m_{\alpha\beta}\sigma_{\beta} = \frac{1}{2\pi\nu_0\tau} \int \frac{d\mathbf{k}}{(2\pi)^2} \hat{G}_{\mathbf{k}+\mathbf{q}}^R\sigma_{\alpha}\hat{G}_{\mathbf{k}}^A\sigma_{\alpha} \tag{15}$$

$$z_{\beta}(\mathbf{q}) = \frac{1}{4\pi\nu_0\tau} \text{Tr} \left[\int \frac{d\mathbf{k}}{(2\pi)^2} \hat{G}_{\mathbf{k}+\mathbf{q}}^R(0) \hat{j}_x\left(\mathbf{k} + \frac{\mathbf{q}}{2}\right) \hat{G}_{\mathbf{k}}^A(0) \sigma_{\beta} \right]. \tag{16}$$

Inverting the matrix equation (14), we find J_{α} and then substituting these in Eq.(11), we obtain σ_{yx}^{AH} .

III. RESULTS AND DISCUSSIONS

In the metallic regime ($\epsilon_F\tau \gg 1$), there is no net σ_{yx}^{AH} when the applied electric field is uniform. When both subbands are partially occupied, the bare bubble contribution

$$\sigma_b^{AH} = -\frac{e^2}{2\pi} \frac{m\alpha^2\Delta_{ex}}{\Delta_{ex}^2 + \Delta_R^2 + \left(\frac{1}{2\tau}\right)^2} \tag{17}$$

is exactly canceled by the ladder vertex correction, σ_v^{AH} , which is numerically equal to σ_b^{AH} but opposite in sign. In the super clean limit ($\tau \rightarrow \infty$), the above value agrees with the previous result¹¹.

In this paper, we are considering the effect of inhomogeneous longitudinal electric field, *i.e.*, $\mathbf{q} \parallel \mathbf{E}_{\mathbf{q}}$ on the Anomalous Hall conductivity. We define three dimensionless parameters out of four energy scales ϵ_F , Δ_R , Δ_{ex} and $1/\tau$. They are $\epsilon_F\tau$, $\Delta_R\tau$ and $\Delta_{ex}\tau$. We numerically calculate σ_{yx}^{AH} for different sets of these parameters given in Table-1, using Eqs. (11), (14)–(16) when the electric field is assumed to be applied along x-axis, *i.e.*, $E_x = E_0 e^{iq_x x}$, $E_y = 0$.

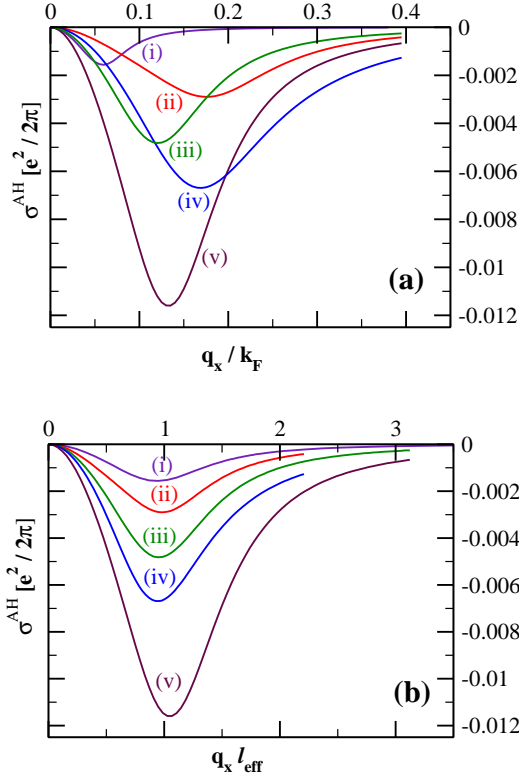


FIG. 2. (Color online) (a) The variation of anomalous Hall conductivity in the unit of $e^2/(2\pi)$ with q_x/k_F for different sets of parameters (i)–(v) shown in Table-1. The peaks in σ^{AH} occur at different values of q_x/k_F depending on the choice of the parameters. Scaling q_x/k_F by $(\epsilon_F\tau)^{-1}(\Delta_{ex}\tau)^{-1/2}$, σ^{AH} is replotted (b) against $q_x l_{eff}$ for all the chosen sets of parameters. Peaks in (b) occur when $q_x l_{eff} \sim 1$.

Set	$\Delta_R\tau$	$\Delta_{ex}\tau$	$\epsilon_F\tau$	$-\sigma_b^{AH} [e^2/(2\pi)]$
(i)	0.2	0.4	10.0	0.0018
(ii)	0.2	0.8	5.0	0.0034
(iii)	0.25	0.4	5.0	0.0061
(iv)	0.2	0.2	2.5	0.0071
(v)	0.4	0.4	5.0	0.0112

TABLE I. Five sets (i)–(v) of three parameters $\Delta_R\tau$, $\Delta_{ex}\tau$, and $\epsilon_F\tau$ used to calculate σ^{AH} for the Fig. (2). The last column shows the value of σ_b^{AH} calculated using Eq.(17) in the unit of $e^2/(2\pi)$ for these sets of parameters.

As evident in Fig.2(a), the magnitude of σ^{AH} increases, forms a peak, and then decreases with the increase of q_x . We note that the peak values for the different sets of parameters are close to the corresponding bare contributions σ_b^{AH} listed in Table-1. This suggests that the effect of inhomogeneous electric field on the AHC is substantial. The peak positions and the maximum values of σ^{AH} depend on these three parameters. However, if we scale q_x in the unit of inverse effective mean free path, $l_{eff} = \sqrt{l_{ex}}$ where $l = v_F\tau$ is the mean free path of an electron and $l_{ex} = v_F/(4\Delta_{ex})$ is the length

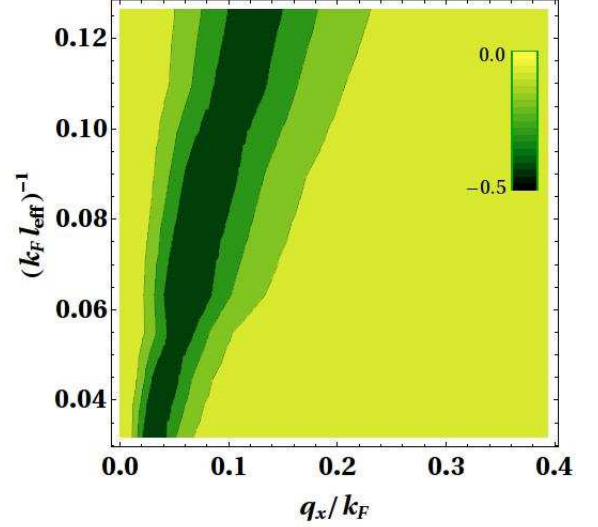


FIG. 3. (Color online) Contour plot of scaled anomalous Hall conductivity, $\tilde{\sigma}^{AH} = \sigma^{AH}(\epsilon_F\tau)(\Delta_R\tau)^{-2}$ versus $\frac{q_x}{k_F}$ and $(k_F l_{eff})^{-1}$. The darkest linear patch, where the magnitude of $\tilde{\sigma}^{AH}$ is maximum, occurs when $q_x l_{eff} \approx 1$.

scale corresponding to the exchange energy, the peak positions occur at $q_x l_{eff} \approx 1$, irrespective of the values of the parameters (see Fig.2(b)). On the other hand, the magnitudes of the peaks depend on two parameters: $\sigma^{AH} \sim (\Delta_R\tau)^2(\epsilon_F\tau)^{-1}$. Figure 3 shows a contour plot of $\tilde{\sigma}^{AH} = \sigma^{AH}(\epsilon_F\tau)(\Delta_R\tau)^{-2}$ as a function of $\frac{q_x}{k_F}$ and $(\Delta_{ex}\tau)^{1/2}(\epsilon_F\tau)^{-1}$, *i.e.*, $(k_F l_{eff})^{-1}$. Note that for the nearly-linear darkest patch, in which the magnitude of $\tilde{\sigma}^{AH}$ is maximum, corresponds to $q_x l_{eff} \approx 1$.

These results suggest that if an electric field of the form $E_x = E_0 e^{iq_x x}$ is applied along the x-axis in the plane of a two dimensional electron gas, the AHC becomes finite. As the maximum magnitude of AHC occurs at $q_x/k_F = (\Delta_{ex}\tau)^{1/2}(\epsilon_F\tau)^{-1}$, the periodic variation of the applied field should be properly tuned in accordance with the relevant parameters of the system to increase the transverse charge current. Clearly, the nature of this periodicity depends on magnetization, disorder and carrier concentration (*i.e.* on Δ_{ex} , τ , and ϵ_F respectively) and *not* on Rashba parameter α . This is illustrated in Fig. 4. An increased variation of the electric field is necessary to produce maximum AHC in a system with higher l_{eff} , *i.e.*, with increasing magnetization and disorder, and decreasing electron density.

IV. SUMMARY

To summarize, we have calculated the anomalous Hall conductivity for a two dimensional ferromagnetic Rashba system with an electric field inhomogeneous in nature. It vanishes for a homogeneous electric field in the weak

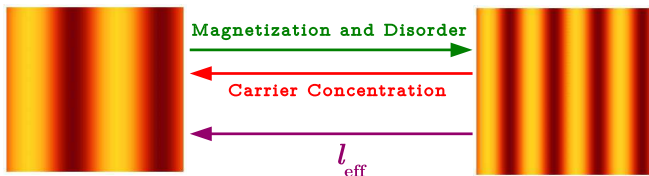


FIG. 4. (Color online) Schematic variation of the inhomogeneous electric field E_x , causing *resonance in AHC*: The periodicity is illustrated by the color gradient. For increased magnetization and disorder and decreased Fermi energy, *i.e.*, for increased l_{eff} , the spatial variation of the electric field should be increased to obtain this resonance.

scattering regime when both the subbands are occupied. We have shown that the anomalous Hall current can increase considerably due to the variation of the electric field and this comes from the bare bubble and ladder vertex correction and *not* from the skew scattering. Dealing with a realistic parameter range, we have found that the length scale associated with the peaks in the conductivity is proportional to the geometric mean of the two length scales arising from disorder and the exchange interaction.

ACKNOWLEDGMENTS

AS acknowledges the assistance provided by the scholars of theoretical physics department of IACS.

-
- ¹ R. Karplus and J. M. Luttinger, Phys. Rev. **95**, 1154 (1954).
 - ² M. V. Berry, Proc. R. Soc. London **392**, 45 (1984).
 - ³ J. Smit, Physica **21**, 877 (1955); Physica **24**, 39 (1958).
 - ⁴ L. Berger, Phys. Rev. B **2**, 4559 (1970).
 - ⁵ N. Nagaosa, J. Sinova, S. Onoda, A. H. MacDonald and N. P. Ong, Rev. Mod. Phys. **82**, 1539 (2010).
 - ⁶ N. A. Sinitsyn, A. H. MacDonald, T. Jungwirth, V. K. Dugaev and Jairo Sinova, Phys. Rev. B **75**, 045315 (2007).
 - ⁷ A. A. Kovalev, K. Vborn and Jairo Sinova, Phys. Rev. B **78**, 041305(R) (2008).
 - ⁸ A. Crepieux and P. Bruno, Phys. Rev. B **64**, 014416 (2001).
 - ⁹ V. K. Dugaev, P. Bruno, M. Taillefumier, B. Canals and C. Lacroix, Phys. Rev. B **71**, 224423 (2005).
 - ¹⁰ J. Inoue, T. Kato, Y. Ishikawa, and H. Itoh, Phys. Rev. Lett. **97**, 046604 (2006).
 - ¹¹ T. S. Nunner, N. A. Sinitsyn, M. F. Borunda, V. K. Dugaev, A. A. Kovalev, Ar. Abanov, C. Timm, T. Jungwirth, J. Inoue, A. H. MacDonald and J. Sinova, Phys. Rev. B **76**, 235312 (2007).
 - ¹² M. Borunda, T. S. Nunner, Thomas Luck, N. A. Sinitsyn, Carsten Timm, J. Wunderlich, T. Jungwirth, A. H. MacDonald and J. Sinova, Phys. Rev. Lett. **99**, 066604 (2007).
 - ¹³ T. Kato, Y. Ishikawa, and H. Itoh and J. Inoue, New Journal of Physics **9**, 350 (2007).
 - ¹⁴ B. Zhou, Phys. Rev. B **81** 075318 (2010).
 - ¹⁵ S. Onoda, N. Sugimoto, N. Nagaosa, Phys. Rev. Lett. **97**, 126602 (2006).
 - ¹⁶ A. A. Kovalev, Y. Tserkovnyak, K. Vborn and Jairo Sinova, Phys. Rev. B **79**, 195129 (2009).
 - ¹⁷ D. Culcer, A. MacDonald and Q. Niu, Phys. Rev. B **68**, 045327 (2003).
 - ¹⁸ S. Y. Liu, Norman J. M. Horing and X. L. Lei, Phys. Rev. B **74**, 165316 (2006).
 - ¹⁹ S. Onoda, N. Sugimoto, N. Nagaosa, Phys. Rev. Lett. **77**, 165103 (2008).
 - ²⁰ J. Inoue, T. Kato, G. E. W. Bauer and L. W. Molenkamp, Semicond. Sci. Technol. **24**, 064003 (2009).
 - ²¹ W. Lee, S. Watauchi, V. L. Miller, R. J. Cava and N. P. Ong, Science **303**, 1647 (2004).
 - ²² P. Schwab, R. Raimondi and C. Gorini, EPL **90**, 67004 (2010).
 - ²³ S. S. Mandal and A. Sensharma, Phys. Rev. B **78**, 205313 (2008).
 - ²⁴ L. E. Ballentine and M. Huberman, J. Phys. C: Solid State Phys. **10**, 4991 (1977).
 - ²⁵ A. Sensharma and S. S. Mandal, J. Phys. Condens. Matter **18**, 7349 (2006).